J Wood Sci (2004) 50:123–129
DOI 10.1007/s10086-003-0538-6

ORIGINAL ARTICLE

Jørgen Lauritzen Jensen · Per-Johan Gustafsson

Shear strength of beam splice joints with glued-in rods

Received: November 11, 2002 / Accepted: March 7, 2003

Abstract Splitting failure in beam splice joints with glued-in rods parallel to grain in endwood subjected to pure shear is considered. A simple theoretical expression based on beam-on-elastic-foundation theory and quasi-non-linear fracture mechanics is presented for calculation of the joint strength. Tests were conducted on jointed beams in a four-point bending test setup in which the joints were located at the point of pure shear force. Hardwood dowels with a diameter of 12 mm and a glued-in length of 120 mm were used as rods, and various beam cross sections and dowel configurations were tested. The theory presented is found to agree well with test results in all cases in which the edge distance of the glued-in rods is relatively small. Some test results indicate that the theory may be conservative in case of large edge distances.

Key words Shear strength · Splice joint · Glued-in rods · Quasi-non-linear fracture mechanics · Beam-on-elastic-foundation

Introduction

Much research on timber joints has recently been dedicated to pull-out of glued-in rods and to the performance of moment-resisting joints with glued-in rods.[1] Hardwood dowels have also been investigated as an alternative to steel rods.[2–5] Beam splice joints subjected to pure bending have previously been tested and simple theoretical expressions for calculation of their strength and stiffness have been presented.[6–9] However, the shear strength of joints with glued-in rods seems not to have been investigated so far.

J.L. Jensen (✉)
Institute of Wood Technology, Akita Prefectural University, Noshiro 016-0876, Japan
Tel. +81-185-52-6985; Fax +81-185-52-6976
e-mail: jensen@iwt.akita-pu.ac.jp

P.-J. Gustafsson
Division of Structural Mechanics, Lund Institute of Technology/Lund University, Lund S-221 00, Sweden

Although glued-in rods are very efficient for making joints with high bending moment capacity, the shear capacity is low unless special actions are taken. In Fig. 1 is shown a shear failure mode in a beam with glued-in rods. Failure occurs as splitting of the beam due to stresses perpendicular to the grain. To make a joint with high moment capacity, the most efficient use of the rods is obtained if they are placed as close as possible to the top and bottom of the beam, i.e., using as small effective edge distance, h_e (as shown in Fig. 1), as possible. However, the shear capacity obviously increases with increasing h_e.

A simple expression is proposed for calculation of the strength of a joint with glued-in rods subjected to pure shear. The expression is derived using beam-on-elastic-foundation theory and quasi nonlinear fracture mechanics. Joints in beams with cross-sectional dimensions of 100 × 200 mm, 50 × 300 mm, and 120 × 420 mm and various dowel configurations were tested in pure shear.

Theory

Introduction

A symmetrical joint as shown in Fig. 1 is considered. Failure occurs as a splitting failure in the beam (mode I fracture of the wood due to tensile stress perpendicular to grain) at the rods located closest to the beam axis as shown in Fig. 1. The part above the crack of the beam to the right of the joint is considered and treated as a beam on elastic foundation. This is a simplifying assumption used in the present theory and may be regarded as a compromise between the strive for simplicity and that of accuracy.

The properties of the elastic foundation are chosen so that the perpendicular-to-grain tensile strength and fracture energy properties of the wood are correctly represented. The analysis is linear elastic, but because strength, fracture energy, and a nonzero size of the fracture process region are considered in the analysis, the analysis may be called a quasi-non-linear fracture mechanics analysis. Results of

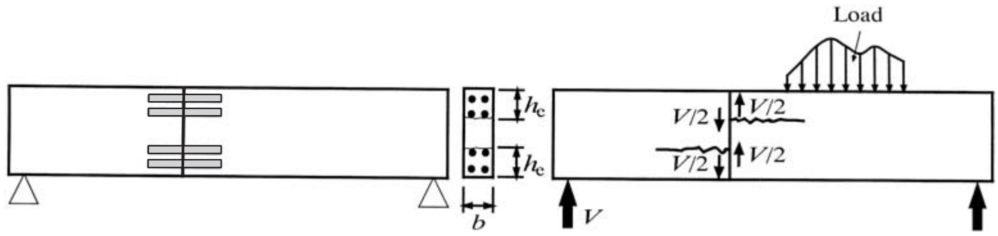

Fig. 1. Splitting failure in a beam with glued-in rods subjected to shear loading

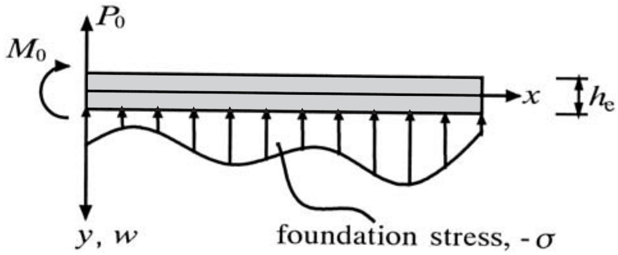

Fig. 2. Semi-infinite beam on elastic foundation

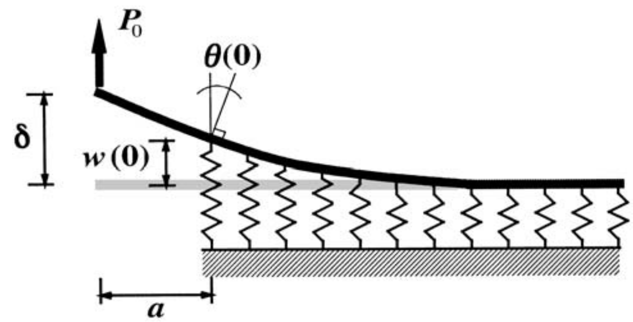

Fig. 3. Beam on elastic foundation after development of a crack of length a

linear elastic fracture mechanics are obtained as a special case by allowing the tensile strength of the wood approach an infinitely large value.

Stress and energy release rate

Figure 2 shows a beam on elastic foundation subjected to a shear force, P_0, and a moment, M_0, at $x = 0$. If the beam is supposed to be infinitely long, and if shear deformations are taken into account, the deflection at $x = 0$, w_0, is given by[10,11]

$$\begin{aligned} w_0 &= w(0) = -\frac{2}{Kb}\left(\beta P_0 + \lambda^2 M_0\right) \\ \beta &= \sqrt{\lambda^2 + \frac{3Kb}{10GA}},\ \lambda^4 = \frac{Kb}{4EI} \end{aligned} \tag{1}$$

where b is the beam width, E is the modulus of elasticity (MOE) in the grain direction of the beam, G is the shear modulus of the beam, K is the stiffness of the elastic foundation (units: N/m^3), I is the moment of inertia, and A is the cross-sectional area of the beam (rectangular cross section is assumed).

The rotation, θ_0, of the beam end at $x = 0$ is given by

$$\theta_0 = \theta(0) = -\frac{P_0}{2EI\lambda^2} - \frac{M_0}{\beta}\left(\frac{6\lambda^2}{5GA} + \frac{1}{EI}\right) \tag{2}$$

The foundation stress acting on the beam (σ), $\sigma > 0$ corresponding to tensile perpendicular-to-grain stress in the wood, is given by

$$\sigma(x) = -Kw(x) \tag{3}$$

Pure shear load, i.e., $M_0 = 0$, is assumed. In this case, maximum deformation and stress occur at $x = 0$. Eqs. 1 and 3 give

$$\sigma(0) = \frac{P_0}{b}\sqrt{4\lambda^2 + \frac{6Kb}{5GA}} \tag{4}$$

The crack propagation energy release rate is denoted by $\mathcal{G}$ and is by definition the release of elastic strain energy and potential energy of loads per unit area of crack extension. For a linear elastic body loaded by a single load, P_0, $\mathcal{G}$ is given by[12]

$$\mathcal{G} = \frac{P_0^2}{2b}\frac{dC}{da} \tag{5}$$

where a is the crack length and C is the compliance given by

$$C = \frac{\delta}{P_0} \tag{6}$$

δ being the deflection at the loading point.

A cantilever beam on elastic foundation, as shown in Fig. 3 (only the beam axis is shown), is considered. The projecting length, a, models the crack in the fracture mechanics analysis. The total deflection, δ, of the loading point may be given as

$$\delta = \delta_a + \delta_w + \delta_\theta \tag{7}$$

where δ_a is the contribution from the projecting cantilever

$$\delta_a = \left(\frac{a^3}{3EI} + \frac{6a}{5GA}\right)P_0 \tag{8}$$

and $\delta_w + \delta_\theta$ is the contribution from the beam on elastic foundation using $M_0 = P_0 a$ in Eqs. 1 and 2

$$\delta_w + \delta_\theta = |w_0| + a|\theta_0| = \left(\frac{\alpha^2}{\beta}\left(\frac{6\lambda^2}{5GA} + \frac{1}{EI}\right) + \frac{a}{EI\lambda^2} + \frac{2\beta}{Kb}\right)P_0 \tag{9}$$

From Eqs. 6–9, the increase in compliance due to an infinitesimal crack extension is found to be

$$\frac{dC}{da} = \frac{a^2}{EI} + \frac{2a}{\beta}\left(\frac{6\lambda^2}{5GA} + \frac{1}{EI}\right) + \frac{1}{EI\lambda^2} + \frac{6}{5GA} \tag{10}$$

Inserting Eq. 10 in Eq. 5, and utilizing the fact that maximum failure load is obtained for $a \to 0$, leads to

$$\mathcal{G} = \frac{P_0^2}{2b}\left(\frac{1}{EI\lambda^2} + \frac{6}{5GA}\right) \tag{11}$$

Comparison of this equation with Eq. 4 shows a simple relation between the maximum stress, $\sigma(0)$, and the energy release rate, $\mathcal{G}$:

$$\mathcal{G} = \frac{(\sigma(0))^2}{2K} \tag{12}$$

Foundation properties and failure criteria

The foundation of the beam is intended to model the strength and fracture performance of the wood perpendicular to the grain. The damage and fracture performance of wood is nonlinear. This nonlinear response is represented in the present analysis by a linear response that is equivalent in terms of peak stress, f_t, and fracture energy dissipation, $\mathcal{G}_f$. The two parameters determine the fracture stress, f_t, and the foundation stiffness, K. Since the energy dissipation in the case of linear performance is

$$\mathcal{G}_f = \frac{1}{2}f_t\left(\frac{f_t}{K}\right) \tag{13}$$

it follows that

$$K = \frac{f_t^2}{2\mathcal{G}_f} \tag{14}$$

The failure load, here denoted as P_c, can be determined by a stress criterion or by an energy release rate criterion. The stress criterion is

$$\sigma(0) = f_t \tag{15}$$

which, by use of Eq. 4, gives

$$P_c = \frac{f_t b}{\sqrt{4\lambda^2 + \frac{6}{5}\frac{Kb}{GA}}} \tag{16}$$

The energy release rate criterion is

$$\mathcal{G} = \mathcal{G}_c \tag{17}$$

where the critical energy release rate, $\mathcal{G}_c$, is the value of $\mathcal{G}$ when a crack is about to start to propagate. Assuming static or quasi-static conditions and no energy dissipation outside the fracture region, $\mathcal{G}_c$ is equal to the material property parameter $\mathcal{G}_f$:

$$\mathcal{G}_c = \mathcal{G}_f \tag{18}$$

From Eq. 18, it follows from Eqs. 11 and 17 that

$$P_c = \frac{b\sqrt{2K\mathcal{G}_f}}{\sqrt{4\lambda^2 + \frac{6}{5}\frac{Kb}{GA}}} \tag{19}$$

The value of P_c by the energy release analysis is the same as the value obtained by the stress analysis because, from Eq. 14, $\sqrt{2K\mathcal{G}_f} = f_t$.

The present strength analysis of mode I failure using beam on elastic foundation and Eq. 14 is a complete analogy to the fracture mechanics application of the Volkersen model to strength analysis of mode II failure in lap joints[13] and pull-out of glued-in rods.[1,5]

Equations for the shear failure load

The shear failure load, $V_{c,L} = 2P_c$, of the symmetrical joint shown in Fig. 1 may, by means of Eq. 16 or 19 together with Eqs. 1 and 14, be written

$$V_{c,L} = 2bl_e f_t, \quad l_e = \frac{h_e}{\sqrt{4\sqrt{3}\omega + \frac{6}{5}\frac{E}{G}\omega^2}}, \quad \omega = \sqrt{\frac{h_e}{E}\frac{f_t^2}{2\mathcal{G}_f}} \tag{20}$$

The length l_e may be interpreted as the equivalent length on both sides of the joint, over which the beam with depth h_e is able to distribute the stresses perpendicular to the grain uniformly.

Equation 20 is based on the present quasi-non-linear fracture mechanics analysis – the stress analysis is linear, at the same time as both limited material strength, nonzero fracture energy, and compliance and nonzero size of the fracture zone are considered. For the special case of linear elastic fracture mechanics analysis, the failure load $V_{c,LEFM}$ is obtained by letting $f_t \to \infty$, or more generally, by letting $\omega \to \infty$, giving

$$V_{c,LEFM} = b\sqrt{\frac{20}{3}G\mathcal{G}_f h_e} \approx 2.58b\sqrt{G\mathcal{G}_f h_e} \tag{21}$$

Equation 20 is based on the assumption that the beam end at the loading point is subjected to a pure shear load and that no rotational restraints are imposed. This is a lower-bound solution because the rotational stiffness of the glued-in dowel group in some cases may be significant as compared with the bending stiffness of the beam on elastic foundation. An upper-bound solution, $V_{c,U}$, is obtained if it is assumed that the rotation of the beam-end is zero at the loading point. Using the following dimensionless parameters

$$\omega = \sqrt{\frac{h_e}{E}\frac{f_t^2}{2\mathcal{G}_f}}$$

$$\zeta = \frac{5}{\sqrt{3}}\frac{G}{E}\frac{1}{\omega}, \quad \nu = \frac{\sqrt{2\zeta+1}}{\zeta+1}, \quad \mu = \frac{\zeta+1}{2\zeta+1} \tag{22}$$

the lower-bound, $V_{c,L}$, and upper-bound, $V_{c,U}$, solutions according to the quasi-non-linear fracture mechanics analysis may be given in terms of the linear elastic fracture mechanics solution, $V_{c,LEFM}$, as shown in Eqs. 23 and 24

$$V_{c,L} = \mu\nu V_{c,LEFM} \tag{23}$$

$$V_{c,U} = \nu V_{c,LEFM} \tag{24}$$

In Fig. 4, the normalized failure loads $\mu = V_{c,L}/V_{c,U}$, $\nu = V_{c,U}/V_{c,LEFM}$, and $\mu\nu = V_{c,L}/V_{c,LEFM}$ are shown as a function of h_e using the material properties $E = 10\,\text{GPa}$, $G = E/18$, $f_t = 4\,\text{MPa}$, $\mathcal{G}_f = 0.25\,\text{N/mm}$. The linear elastic fracture mechanics solution as given by Eq. 21 is seen to be a fairly good approximation to the quasi-non-linear fracture mechanics upper-bound solution for most practical situations. It is worth noting that for $h_e \to 0$ (or more generally, $\omega \to 0$): $\nu = V_{c,U}/V_{c,LEFM} \to 0$ and $\mu = V_{c,L}/V_{c,U} \to 1/2$. For $h_e \to \infty$ (or more generally, $\omega \to \infty$): $\nu = V_{c,U}/V_{c,LEFM} \to 1$ and $\mu = V_{c,L}/V_{c,U} \to 1$.

The factors ν and $\mu\nu$ maybe interpreted as effectiveness factors by which the linear elastic fracture mechanics solution (Eq. 21) is multiplied in order to obtain the quasi-non-linear fracture mechanics solutions. As indicated by Fig. 4, a simple and practical approach may be to determine the effectiveness factors for a certain minimum allowable value of h_e, which will then be a safe value for all allowable h_e.

The quasi-non-linear fracture mechanics solutions given by Eqs. 21–24 depend in general on the tensile strength perpendicular to the grain, f_t, which is highly volume dependent and difficult to estimate appropriately by testing. For a problem such as the one considered here, the crack propagation path is predetermined and the tensile strength should thus be determined using specimens with a very small volume. Furthermore, tensile strength tests will always give a lower-bound estimate since misalignments inevitably cause nonuniform stress distribution. The use of tensile strength as determined by testing will therefore, in the present context, in general be on the safe side.

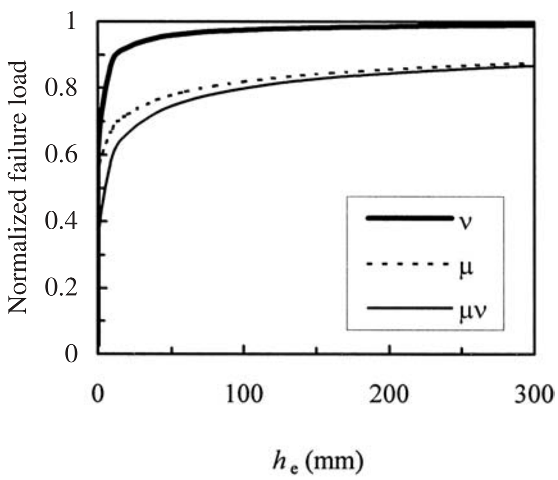

Fig. 4. Normalized failure loads $\nu = V_{c,U}/V_{c,LEFM}$, $\mu = V_{c,L}/V_{c,U}$, and $\mu\nu = V_{c,L}/V_{c,LEFM}$ as functions of effective beam depth h_e

Experimental

Tests were conducted in a test setup, as shown in Fig. 5, that provided pure shear at the location of the joint. The geometry of the eight kinds of joints tested is shown in Fig. 6. The effective beam depth, h_e, shown in Fig. 6, is taken as $h_e = h_c + \frac{1}{2}d$, where h_c is the distance from the loaded edge of the beam to the center of the innermost row of dowels, and d is the dowel diameter.

The glulam beams (30mm laminae) used in the testing program were made of Japanese cedar (*Cryptomeria japonica*), and ordered from the factory as E75-F240 according to the Japanese Agricultural Standard.[14] The dynamic modulus of elasticity (MOE) was determined for each beam, and is given in Table 2 as the mean value for each test series. The moisture content (MC) of the glulam was between 12% and 13%, and the density was about $420\,\text{kg/m}^3$ at the given MC.

The dowels were made of hard maple (*Acer saccharum*). The dowel diameter was 12mm, and the glued-in length was 120mm (in each beam end) in all specimens except specimens A1 and A2, in which staggered glued-in lengths were used (longest dowels in the outer laminae, shortest dowels in the row closest to the beam axis). Specimen A1 contained three dowel rows with glued-in lengths of 120, 110, and 100mm. Specimen A2 contained five dowel rows with glued-in lengths of 120, 110, 100, 90, and 80mm. The dowel surface was smooth without grooves, and the dowel holes were 13mm in diameter. The MOE of the hardwood was about 15GPa, the MC was about 11%, and the density was about $740\,\text{kg/m}^3$ at the given MC.

The adhesive used was one-component polyurethane C3060 (Nihon Polyurethane) or #930 (Sunstar Engineering). Previous pull-out tests showed no significant difference in strength between the two adhesives. Curing time, i.e., the time from gluing to testing, ranged from 4 to 14

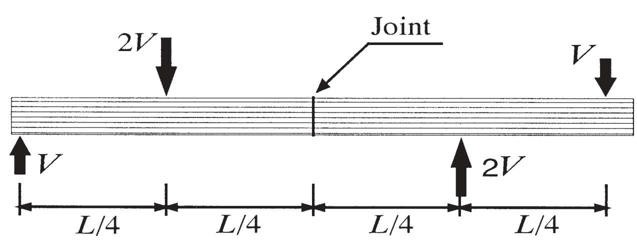

Fig. 5. Test setup for joints subjected to pure shear

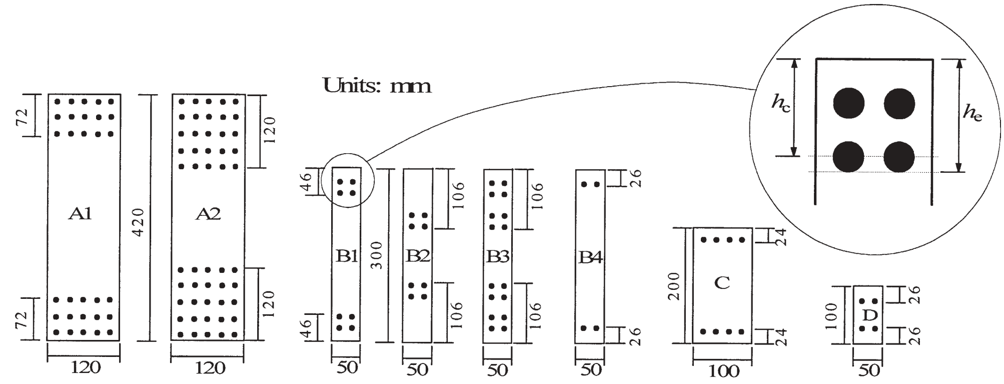

Fig. 6. Geometry of joints with glued-in hardwood dowels tested in pure shear

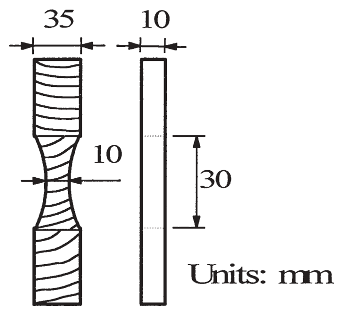

Fig. 7. Specimen for determination of tensile strength perpendicular to grain

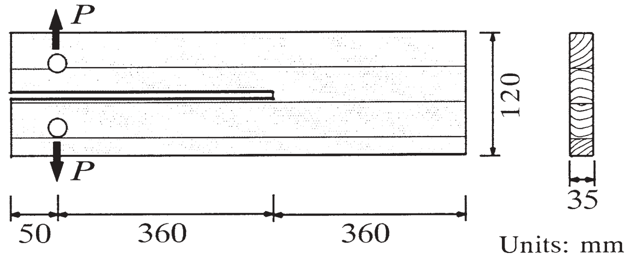

Fig. 8. DCB specimen for determination of fracture energy

days. The glulam beams and the dowels, as well as the specimens after gluing, were stored in the laboratory without controlling temperature or humidity.

The dowels were glued into the beams simply by injecting adhesive into the dowel holes and pressing the dowels into the holes. In some cases, excessive adhesive was pushed out and provided the potential to create a bond between the end surfaces of the jointed beams. In order to avoid transfer of shear forces through such a bond line (i.e., to ensure transfer of shear forces through the dowels only), a 3-mm to 6-mm gap was deliberately made between the end surfaces of the jointed beams, and a double layer of plastic film was placed in the gap.

Tests were also conducted to determine tensile strength perpendicular to the grain and fracture energy of the wood in some of the glulam beams. The tensile strength was determined using specimens as shown in Fig. 7, and the fracture energy was determined using Double-Cantilever-Beam (DCB) specimens as shown in Fig. 8 (the 120-mm wide glulam beams were cut into three 35-mm wide specimens labeled A, B, C). The material for tensile strength specimens and DCB specimens was taken without special selection to avoid defects such as knots.

The fracture energy, assumed to equal the critical energy release rate, was calculated from the recorded failure load, P_{max}, by[15]

$$\mathcal{G}_f = \frac{P_{max}^2}{bEI}\left(a + \sqrt{\frac{6EI}{5GA}}\right)^2 \tag{25}$$

Table 1. Tensile strength and fracture energy perpendicular to grain

Specimen	MOE (MPa)	f_t (MPa)	$\mathcal{G}_f$ (N/mm)
B07-A	8817	4.0	0.17
B07-B	8817	5.3	0.24
B07-C	8817	3.6	0.16
B08-A	8612	6.2	0.33
B08-B	8612	6.5	0.61
B08-C	8612	3.0	0.36
B09-A	8660	4.2	0.24
B09-B	8660	–	0.35
B09-C	8660	3.2	0.20
B10-A	9288	2.8	0.18
B10-B	9288	3.8	0.15
B10-C	9288	3.4	0.22
B11-A	8324	3.6	0.24
B11-B	8324	2.9	0.58
B11-C	8324	3.3	0.14
B12-A	9504	3.6	0.19
B12-B	9504	6.9	0.39
B12-C	9504	4.2	0.27
Mean ± SD	8868 ± 445	4.1 ± 1.3	0.28 ± 0.14

Calculation of $\mathcal{G}_f$ based on $\mathcal{G}_f = \mathcal{G}_c$ and $G = E/18$
MOE, Modulus of elasticity; f_t, fracture stress; $\mathcal{G}_f$, fracture energy dissipation

where A and I are cross-sectional area and moment of inertia, respectively, of a cantilever, and a is the initial crack length ($a = 360\,\text{mm}$).

Results and discussion

The specimens for determination of the tensile strength perpendicular to the grain and the DCB specimens were cut

Table 2. Failure shear load of joints subjected to pure shear

Specimen	MOE (MPa)	b (mm)	h_e (mm)	V_c (kN)			
				Test	Eq. 23	Eq. 24	Eq. 21
A1-01	8670	120	72	30.2			
A1-02	8670	120	72	28.2			
A1-03	8670	120	72	36.2			
Mean ± SD	8670	120	72	31.5 ± 4.2	23.8	29.6	30.5
A2-01	8670	120	120	43.2			
A2-02	8670	120	120	66.0			
A2-03	8670	120	120	48.2			
A2-04	9950	120	120	46.8			
A2-05	9950	120	120	55.6			
A2-06	9950	120	120	48.1			
Mean ± SD	9310	120	120	51.3 ± 8.2	33.1	40.0	40.8
B1-01	8340	50	46	8.1			
B1-02	8340	50	46	7.3			
B1-03	8340	50	46	6.4			
Mean ± SD	8340	50	46	7.3 ± 0.9	7.5	9.6	10.0
B2-01	8340	50	106	10.9			
B2-02	8340	50	106	12.5			
B2-03	8340	50	106	15.3			
Mean ± SD	8340	50	106	12.9 ± 2.2	12.3	14.8	15.1
B3-01	9950	50	106	23.6			
B3-02	9950	50	106	22.0			
B3-03	9950	50	106	18.5			
B3-04	9950	50	106	20.5			
B3-05	9950	50	106	15.3			
B3-06	9950	50	106	19.1			
Mean ± SD	9950	50	106	19.8 ± 2.9	13.2	16.1	16.5
B4-01	9950	50	26	6.5			
B4-02	9950	50	26	7.6			
B4-03	9950	50	26	6.9			
Mean ± SD	9950	50	26	7.0 ± 0.6	5.6	7.6	8.2
C-01	8340	100	24	12.4			
C-02	8340	100	24	9.2			
C-03	8340	100	24	10.4			
C-04	8340	100	24	10.8			
C-05	8250	100	24	12.5			
C-06	8250	100	24	11.7			
C-07	8250	100	24	10.1			
Mean ± SD	8300	100	24	11.0 ± 1.2	10.0	13.5	14.4
D-01	9950	50	26	6.1			
D-02	9950	50	26	7.0			
D-03	9950	50	26	7.7			
Mean ± SD	9950	50	26	6.9 ± 0.8	5.6	7.6	8.2

Calculations based on $G = E/18$, $f_t = 4.1$ MPa, and $\mathcal{G}_f = 0.28$ N/mm
b, Beam width; h_e, beam depth; V_c, failure shear load

from the A2-01, A2-02, and A2-03 specimens (Fig. 6), which were composed of the six beams B07–B12. In Table 1, the tensile strength and fracture energy perpendicular to the grain are given along with the measured MOE (the MOE given in Table 2 for the same specimens is the mean value of the six beams reported in Table 1 and the six beams used for specimens A1).

The results in Table 1 show a large variation even among neighboring specimens taken from the same beam (A, B, C) due to the presence of knots, which have a reinforcing effect. Tests on clear specimens therefore tend to underestimate the critical energy release rate. On the other hand, as is obvious from Table 1, the reinforcing effect of small knots may be very localized. A small knot that has a significant reinforcing effect on a 35-mm wide DCB specimen may not necessarily lead to reinforcement of the 120-mm wide cross section. For practical use, it is therefore recommended that either specimens without knots in the vicinity of the crack tip or specimens with a full-size width be used for determination of the critical energy release rate.

The results of the pure shear tests of the joints are given in Table 2 and are compared with the calculated failure loads according to the linear elastic fracture mechanics solution, as given by Eq. 21, and the quasi-non-linear lower-bound and upper-bound solutions as given by Eqs. 23 and 24, respectively.

The B4 and D specimens were tested in order to observe the effect of beam depth, h, for constant h_e. Though the present test results are too sparse to make any final conclusions, they seem to suggest that the failure load depends on h_e, but is not affected by the total beam depth, h. The fracture mechanics model presented is in agreement with this finding. Comparison of specimens B2 and B3 suggests that the rotational restraint has a significant effect.

The test results of specimens A2 and B3 show significantly higher strength than theoretically expected. All other theoretically estimated strengths are in good agreement with test results. This might indicate that the theory presented here is particularly suited to joints with relatively small edge distances (e.g., $h_e/h < 0.2$), which is most common in practice, while it is somewhat conservative for large edge distances. However, the reported test data are too sparse to make final conclusions. Further tests should be conducted to clarify the validity range of the theory.

Conclusions

A theoretical model based on beam-on-elastic-foundation theory and quasi-non-linear fracture mechanics was proposed for calculation of the failure shear load of beam splice joints with rods glued in parallel to the grain direction and which fail in splitting due to tensile stresses perpendicular to the grain. Theoretical failure shear loads were, for the majority of the test series, found to be in good agreement with test results. This seems to be particularly so for test series with relatively small edge distances, while test results of two test series with relatively large edge distances showed considerably higher failure loads than expected from the theory, indicating that the presented theory may be somewhat conservative in case of large edge distance. Further tests should be conducted to clarify the validity range of the theory. The present theory is approximate because of the simplifying assumptions made. A more accurate theory, involving more complicated calculations, may be developed by taking into account the bending and shear deformations of the part of the beam below the crack path, which in the present theory is treated as a fixed foundation. The simplicity of the present theory makes it suitable for practical design.

References

1. Gustafsson PJ, Serrano E (2001) Glued-in rods for timber structures – development of a calculation model. Report TVSM-3056, Division of Structural Mechanics, Lund University, Sweden
2. Koizumi A, Jensen JL, Sasaki T, Iijima Y, Tamura Y (1998) Withdrawal properties of hardwood dowels in end joints I. Evaluation of shear performance of adhesives (in Japanese). Mokuzai Gakkaishi 44:41–48
3. Koizumi A, Jensen JL, Sasaki T, Iijima Y, Tamura Y (1998) Withdrawal properties of hardwood dowels in end joints II. Effects of dowel diameters, Young's moduli of adherends, dowel spacings and numbers of dowels (in Japanese). Mokuzai Gakkaishi 44:109–115
4. Koizumi A, Jensen JL, Sasaki T, Iijima Y, Matsuki Y, Komatsu K (1999) Withdrawal properties of hardwood dowels glued in perpendicular to the grain (in Japanese). Mokuzai Gakkaishi 45:230–236
5. Jensen JL, Koizumi A, Sasaki T, Tamura Y, Iijima Y (2001) Axially loaded glued-in hardwood dowels. Wood Sci Technol 35:73–83
6. Komatsu K, Koizumi A, Sasaki T, Jensen JL, Iijima Y (1997) Flexural behavior of GLT beams end-jointed by glued-in hardwood dowels. In: Proceedings of the international council for building research studies and documentation, CIB W18A, Meeting 30, Vancouver, Canada, pp 1–8
7. Sasaki T, Koizumi A, Jensen JL, Iijima Y, Tamura Y, Komatsu K (1999) End joint with glued-in hardwood dowels in timber construction I. Bending properties of beams jointed with single row of dowels (in Japanese). Mokuzai Gakkaishi 45:17–24
8. Sasaki T, Koizumi A, Jensen JL, Iijima Y, Komatsu K (2002) End joint with glued-in hardwood dowels in timber construction II. Bending properties of beams jointed with multiple rows of dowels (in Japanese). Mokuzai Gakkaishi 48:23–31
9. Jensen JL, Koizumi A, Sasaki T (1999) Timber joints with glued-in hardwood dowels. In: Proceedings of pacific timber engineering conference, PTEC'99, Rotorua, New Zealand. Forest Research Bulletin 212, vol. 2, pp 100–107
10. Jorissen AJM (1998) Double shear timber connections with dowel type fasteners. Delft University Press, Delft, The Netherlands
11. Pilkey WD (1994) Formulas for stress, strain, and structural matrices. Wiley, New York, USA, pp 534–545
12. Hellan K (1984) Introduction to fracture mechanics. McGraw-Hill, New York, USA, pp 49–72
13. Gustafsson PJ (1987) Analysis of generalized Volkersen-joints in terms of non-linear fracture mechanics. In: Mechanical behaviour of adhesive joints. Pluralis, Paris, France, pp 323–338
14. Ministry of Agriculture, Forestry and Fisheries (1996) Japanese agricultural standard for glued laminated timber
15. Gustafsson PJ, Larsen HJ (2001) Dowel joints loaded perpendicular to grain. In: Aicher S, Reinhardt HW (eds) Joints in timber structures, RILEM Proceedings PRO 22, pp 577–586